THE JOURNAL OF PHYSICAL CHEMISTRY B

ARTICLE

pubs.acs.org/JPCB

Thermodynamics of Molecular Recognition of mRNA 5′ Cap by Yeast Eukaryotic Initiation Factor 4E

Katarzyna Kiraga-Motoszko,[†] Anna Niedzwiecka,*[,†,‡] Anna Modrak-Wojcik,[†] Janusz Stepinski,[†] Edward Darzynkiewicz,[†] and Ryszard Stolarski[†]

[†]Division of Biophysics, Institute of Experimental Physics, Faculty of Physics, University of Warsaw, 02-089 Warsaw, Poland

[‡]Laboratory of Biological Physics, Institute of Physics, Polish Academy of Sciences, 02-668 Warsaw, Poland

ABSTRACT: Molecular mechanisms underlying the recognition of the mRNA 5′ terminal structure called "cap" by the eukaryotic initiation factor 4E (eIF4E) are crucial for cap-dependent translation. To gain a deeper insight into how the yeast eIF4E interacts with the cap structure, isothermal titration calorimetry and the van't Hoff analysis based on intrinsic protein fluorescence quenching upon titration with a series of chemical cap analogs were performed, providing a consistent thermodynamic description of the binding process in solution. Equilibrium association constants together with thermodynamic parameters revealed similarities and differences between yeast and mammalian eIF4Es. The yeast eIF4E complex formation was enthalpy-driven and entropy-opposed for each cap analog at 293 K. A nontrivial isothermal enthalpy−entropy compensation was found, described by a compensation temperature, T_c = 411 ± 18 K. For a low affinity analog, 7-methylguanosine monophosphate, a heat capacity change was detected, ΔC_p° = +5.2 ± 1.3 kJ·mol^{-1}·K^{-1}. The charge-related interactions involving the 5′-5′ triphosphate bridge of the cap and basic amino acid side chains at the yeast eIF4E cap-binding site were significantly weaker (by $\Delta\Delta H^\circ_{vH}$ of about +10 kJ·mol^{-1}) than those for the mammalian homologues, suggesting their optimization during the evolution.

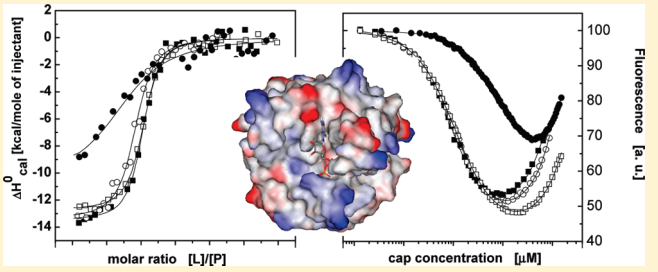

INTRODUCTION

Thermodynamic analysis proved to be an efficient approach for understanding the biophysical bases of forming of intermolecular complexes in aqueous solutions, provided that all thermodynamically coupled processes, e.g., proton, ion, or water exchange, are concurrently taken into account,[1,2] because these accompanying reactions can contribute to apparently contradictory values of thermodynamic parameters determined by isothermal titration calorimetry and the van't Hoff method.[3−5] Recently, thermodynamic analysis was successfully applied to study complex processes, such as self-assembling of membrane proteins,[6] amyloid β-peptide 42 interactions,[7] and antigen−antibody recognition.[8]

A 5′-terminal cap structure (Figure 1b), in which 7-methylguanosine is linked by a 5′,5′-triphosphate bridge to the first transcribed nucleoside of the polynucleotide chain[9] is present in eukaryotic mRNAs, snoRNAs, and TER1. Most snRNAs and nematode mRNAs contain a hypermethylated cap structure $m_3^{2,2,7}$G (5′)ppp(5′)N.[10] Some of the eIF4E isoforms from nematodes and flatworms recognize both types of the cap.[11−14] The mRNA 5′ cap plays a pivotal role in initiation of the cap-dependent translation,[15] protects mRNA against nucleolytic degradation,[16] promotes splicing of mRNA precursors,[17] and facilitates RNA nuclear export.[18] Recognition and binding of the cap by eIF4E during the formation of the 48S preinitiation complex is a rate-limiting step for the cap-dependent translation.[19] Recent studies have shown that the eIF4E activity, both in the cytoplasm and in the nucleus, has a strong impact on the cell cycle progression and cellular proliferation (reviewed, e.g., by Culjkovic et al.[20]).

Overexpression of eIF4E has a profound effect on cell growth and phenotype, leading to an accelerated cell division and tumors, while suppression of eIF4E inhibits cell growth and malignant transformation.[21−24] Aberrations in the level of expression and activity of eIF4E can also change cell morphology. Mammals are more sensitive to such aberrations than yeast, probably due to differences in the mechanism of recruitment of mRNA to the 48S preinitiation complex,[25] and this can also be related to structural and functional differences in eIF4E homologues and isoforms from various sources.

The eIF4E amino acid sequence is highly conserved, with a 29% identity and 44% similarity between yeast and human. The 3D structures of mouse eIF4E bound to m^{7}GDP[26] and m^{7}GpppG,[27] and human eIF4E in complexes with m^{7}GTP and m^{7}GpppA[28] were solved by X-ray diffraction, and the yeast eIF4E-m^{7}GDP complex structure was derived from multidimensional NMR in solution.[29] A structure of eIF4E from wheat was obtained by combination of X-ray crystallography and NMR and revealed an intramolecular disulfide bridge between two cysteins, Cys113 and Cys151, conserved only in plants.[30] Although all

Received: February 5, 2011
Revised: May 14, 2011
Published: June 08, 2011

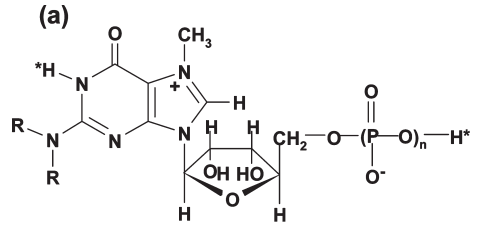

	R	n
m^7GMP	H	1
m^7GDP	H	2
m^7GTP	H	3
$m_3^{2,2,7}GTP$	CH_3	3

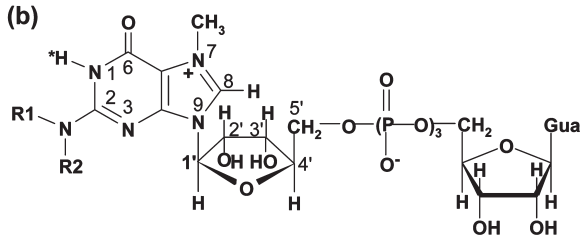

	R1	R2
m^7GpppG	H	H
$m_2^{2,7}GpppG$	H	CH_3
$m_3^{2,2,7}GpppG$	CH_3	CH_3

Figure 1. Structures of (a) mono- and (b) dinucleotide cap analogs. Asterisks denote protons that partially dissociate at pH 7.2. The positive charge at 7-methylguanosine is localized at N(7).[42]

eIF4Es investigated to date exhibit similar tertiary folds and have similar key amino acids in the cap-binding centers, some distinct features are observed among contacts stabilizing the complexes; e.g., the orientation of the tryptophan indole rings stacked with the 7-methylguanine moiety differs significantly in yeast and mammalian eIF4E.[26,29]

Mammalian eIF4E proteins without a bound ligand are thermodynamically unstable and prone to aggregation.[27,31] Progressive deaggregation of mouse eIF4E(33-218) occurs upon interactions with the cap analogs, depending on their eIF4E binding affinity.[31] The cap-bound eIF4E becomes more stiff[32] and resistant against degradation.[33] Cap binding induces changes in the dynamics of the tertiary structure of human[34] and mouse[35] eIF4Es not only in the vicinity of the cap-binding slot but also close to the eIF4G/4E-BP binding site located on the opposite side of the protein.

On the basis of the NMR spectra, the apo-form of yeast eIF4E was postulated to have extensive unstructured regions, which were supposed to be triggered to fold upon binding to the cap or another translation initiation factor, eIF4G.[36] However, the observed changes of signal broadening and distribution in the $^{15}N/^{1}H$ HSQC spectra could be interpreted rather as an aggregation−deaggregation transition[31] instead of local folding of some protein regions, because CD spectra of both yeast[37] and human[34] eIF4E point to lack of substantial changes of the secondary structure content upon the cap binding.

In the context of evolution of cap-dependent translation, it is interesting to compare molecular mechanisms of the cap binding by eIF4Es from various organisms. Previously, we have analyzed the mRNA 5′ cap interaction with mammalian eIF4E.[27,32,38] The goal of this study was to obtain a thermodynamic insight into the cap recognition by *Saccharomyces cerevisiae* eIF4E. We carried out isothermal titration calorimetry (ITC) experiments and fluorescence titrations of eIF4E on the basis of the intrinsic protein fluorescence quenching upon interaction with a series of chemically synthesized cap analogs. Thermodynamic parameters obtained from calorimetry and the van't Hoff method reflect both similarities and differences in the mode of the cap stabilization inside the binding pockets of yeast and mammalian eIF4Es and can be helpful in unraveling the development of the cap-binding strategy adopted by the 4E factors from various species.

EXPERIMENTAL METHODS

Chemical Syntheses. Cap analogs (Figure 1) were synthesized as described previously.[39−41] All used chemicals were analytically pure (Sigma-Aldrich, Merck, or Carl Roth).

Protein Expression and Purification. Recombinant His-tagged yeast eIF4E was expressed in *Escherichia coli*, strain M15 (pREP 4, Qiagen), grown at 37 °C to OD_{280} = 0.6, and induced by 0.5 mM isopropyl thiogalactoside with 0.05 mM phenylmethylsulfonyl fluoride for 4 h at 23 °C. The cells were harvested, frozen in liquid nitrogen, suspended in lysis buffer, 50 mM HEPES/KOH, 300 mM KCl, and 15 mM imidazole, pH 7.2, sonicated, and centrifuged. The protein was purified from the soluble fraction by Ni^{2+}-affinity chromatography on NiNTA resin (Novagen) followed by dialysis against imidazole and KCl at 250 mM to 0 mM and 300 mM to 80 mM, respectively. Next, FPLC was carried out on a 5 mL HiTrap SP column (Pharmacia Biotech) with the KCl gradient, 0.1−1 M. Freshly prepared protein was used for ITC and fluorescence measurements.

Fluorescence Titrations. Absorption spectra were recorded on Lambda 20 UV/vis (Perkin-Elmer Co). Fluorescence spectra were run on LS-50B (Perkin-Elmer Co.) in a quartz semimicro cuvette (Hellma, Germany) with a magnetic stirrer and optical lengths of 4 mm and 10 mm for absorption and emission, respectively. Titration experiments were performed for yeast eIF4E at 0.3 μM, as described previously,[43] in 50 mM HEPES/KOH, 100 mM KCl, and 1 mM EDTA. Buffers were adjusted to pH 7.20 ± 0.01 (Beckman Φ300 pH-meter) with constant ionic strength maintained at each temperature. Temperature stability was better than 0.2 K. The fluorescence raw data were rigorously corrected for the *inner filter* effect, as described previously.[27,43]

Theoretical curve for the fluorescence intensity (F) as a function of the total ligand concentration ([L]) was fitted to the experimental data points according to the equation

$$F = F(0) - [cx](\Delta\phi + \phi_{lig\text{-}free}) + [L]\phi_{lig\text{-}free} \quad (1)$$

where the equilibrium concentration of the protein−ligand complex is

$$[cx] = \frac{[L] + [P_{act}]}{2} + \frac{1 - \sqrt{(K_{as}([L] - [P_{act}]) + 1)^2 + 4K_{as} \cdot [P_{act}]}}{2K_{as}} \quad (2)$$

$F(0)$ is the initial fluorescence intensity of the protein, $\Delta\varphi = \varphi_{P_{act}free} - \varphi_{cx}$ is the difference between the fluorescence efficiencies of the apo-protein and the complex, $\varphi_{lig\text{-}free}$ is the fluorescence efficiency of the free ligand, $[P_{act}]$ is the total concentration

of the active protein, and K_{as} is the equilibrium association constant. The final K_{as} values and the experimental errors were calculated from at least three independent titration runs.[43]

Thermodynamic Parameters from van't Hoff Analysis. The Gibbs free energy of binding (ΔG°) was calculated as

$$\Delta G^\circ = -RT \cdot ln\, K_{as} \quad (3)$$

where R is the gas constant and T is the absolute temperature. Symbols with "°" refer to the pseudostandard state at concentrations of unit molarity.

The temperature dependence of the spectroscopically determined K_{as} was analyzed according to the van't Hoff isobaric equation as a function ln K_{as} (T^{-1}), either as

$$ln\, K_{as} = \frac{\Delta S^\circ}{R} - \frac{\Delta H^\circ_{vH}}{RT} \quad (4)$$

with the standard molar entropy (ΔS°) and van't Hoff enthalpy (ΔH°_{vH}) of binding fitted as free parameters, or in the nonlinear form,[44] as described previously:[38]

$$ln\, K_{as} = \frac{\Delta C^\circ_p}{R}\left[\frac{T_H}{T} - ln\left(\frac{T_S}{T}\right) - 1\right] \quad (5)$$

where the standard molar heat capacity change at constant pressure (ΔC°_p) and the characteristic temperatures (T_S where $\Delta S^\circ = 0$, and T_H where $\Delta H^\circ_{vH} = 0$) were fitted as free parameters, providing ΔS° and ΔH°_{vH}, as follows:

$$\Delta S^\circ = \Delta C^\circ_p\, ln\left(\frac{T}{T_S}\right) \quad (6)$$

$$\Delta H^\circ_{vH} = \Delta C^\circ_p (T - T_H) \quad (7)$$

Isothermal Titration Calorimetry (ITC). Measurements were performed at 293 K on an OMEGA Ultrasensitive titration calorimeter (Micro-Cal), calibrated by titration of 18-crown-6 with $BaCl_2$ in 50 mM HEPES/KOH pH 7.2, 100 mM KCl, and 1 mM EDTA. The eIF4E sample was dialyzed against the buffer by 4-fold centrifugation on 5 kDa Centricon filters (Millipore). After the last centrifugation, the flow-through buffer was collected to fill the reference cell, to dissolve the cap-analogs, and to control for the ligand dilution. The sample was degassed and filtered through a 22 μm filter (Millipore) directly before measurements. The protein concentration of each solution was estimated from absorption. The absorption spectra of the final mixture after each ITC run were measured as a control for the cap concentration. The concentrations were optimized to match a 2.5−3.5-fold excess of the cap over eIF4E in the final mixture and varied from 0.32 to 1 mM of the cap in a 140 μL volume syringe, and from 6 to 20 μM of eIF4E in the reaction cell (V_0 = 1386 μL). The temperature equilibration prior to the experiments was 40 min. A single titration experiment consisted of 1 μL initial injection followed by 34 injections of 4 μL with 300 s time intervals. Slow stirring of 120 rpm was applied to avoid the protein precipitation. The ligand solution was injected to the pure buffer to measure the heat of dilution, which was subtracted from the apparent heat of the complex formation.

Calorimetric data analysis was carried out using Origin ITC software package (Micro-Cal, USA) to determine K_{as}, ΔH°_{cal}, and the active protein concentration. The heat required to keep isothermal conditions during a single injection was derived by integration of the power signal vs. time. The total heat, Q, released in the active volume of the calorimetric cell at a fractional saturation, Θ, of the protein by the ligand is

$$Q = H^\circ_{cal} N[P]\Theta V_0 \quad (8)$$

where ΔH°_{cal} is the total molar calorimetric enthalpy change upon the ligand binding, N is the number of binding sites in the protein molecule, and [P] is the total protein concentration. If the cap binds only to the active eIF4E at a total concentration of [P_{act}],

$$\Theta N[P] = \Theta[P_{act}] = [cx] \quad (9)$$

where [cx] is the complex concentration. The parameters of interest, ΔH°_{cal}, [P_{act}], and K_{as}, were obtained by fitting the titration data to the differential heat of the ith injection as a function of the ligand-to-protein molar ratio, [L]/[P], corrected for dilution and for the heat related to the part of the solution displaced from the active volume of the reaction cell:

$$Q_i - Q_{i-1} = \Delta H^\circ_{cal} N[P] V_0 (\Theta_i - \Theta_{i-1}) \quad (10)$$

The fitted parameter describing the reaction stoichiometry, N, varied from 0.92 to 0.95 in all ITC experiments.

The calorimetric standard molar entropy change was determined as

$$\Delta S^\circ = \frac{\Delta H^\circ_{cal} - \Delta G^\circ}{T} = \frac{\Delta H^\circ_{cal}}{T} + R \cdot ln\, K_{as} \quad (11)$$

Buffer Ionization Heat. ΔH°_{ion} for m^7GTP binding to eIF4E at pH 7.2 were calculated as follows:

$$\Delta H^\circ_{ion} = \frac{10^{-pK_a}}{10^{-pK_a} + 10^{-pH}} \cdot \Delta H^\circ_{H-diss} \quad (12)$$

from the temperature-dependent molar ionization heat for HEPES, $\Delta H^\circ_{H\text{-}diss}$ = +20.95 kJ·mol^{-1} at 298.2 K, with $\delta \Delta H_{H\text{-}diss}{}^\circ/\delta T$ = +0.0648 kJ·mol^{-1}·K^{-1},[45] and the pK_a value for m^7GTP determined by UV absorption spectroscopy as 7.50 ± 0.05.

Computational Analyses. Numerical regressions were carried out by means of a nonlinear, least-squares fitting using Origin 6.0 or OriginPro 7.5 (Microcal Software Inc.), taking into account the experimental uncertainties of the individual data points, weighed by $1/\sigma^2$.

Structural alignment was obtained by Swiss-PdbViewer v4.0.1 for the C^α atoms of the representative yeast eIF4E (1ap8[29]) OLDERADO structure[46] and mouse eIF4E crystal structure (1ej1[26]).

Molecular electrostatic potential surfaces for yeast and mouse eIF4E were calculated by Accelrys DS Visualizer v2.0.1.734. Hydrogens were added to the mouse eIF4E crystal structure before calculating the electrostatic potential surfaces.

RESULTS AND DISCUSSION

Affinity of Yeast eIF4E for the mRNA 5′ Cap. Isothermal titration calorimetry experiments allowed us to determine directly the equilibrium association constants, K_{as}, and the total standard molar calorimetric enthalpy changes, ΔH°_{cal}, related to the association of mRNA 5′ cap analogs, m^7GMP, m^7GDP, m^7GTP, and m^7GpppG (Figure 1) with the yeast translation factor eIF4E (Table 1). Parallelly, fluorescence titration experiments based on intrinsic protein fluorescence quenching upon ligand binding yielded the spectroscopic K_{as} values (Table 2). The standard molar van't Hoff enthalpy changes, ΔH°_{vH}, for two selected analogs of different affinity for eIF4E, m^7GMP and

Table 1. Thermodynamic Parameters for Binding of Cap Analogs to Yeast eIF4E Determined by Isothermal Titration Calorimetry[a]

cap analog	K_{as} (μM^{-1})	$\Delta G°$ (kJ·mol^{-1})	$\Delta H°$ (kJ·mol^{-1})	$\Delta S°$ (J·mol^{-1}·K^{-1})
m^{7}GMP	0.65 ± 0.12	−32.61 ± 0.45	−38.1 ± 1.7	−18.7 ± 6.0
m^{7}GDP	4.7 ± 1.3	−37.43 ± 0.68	−56.9 ± 2.5	−66.4 ± 8.8
m^{7}GTP	6.3 ± 3.2[b]	−38.1 ± 1.2	−56.30 ± 0.25	−62.1 ± 4.2
m^{7}GpppG	3.66 ± 0.68	−36.82 ± 0.45	−54.2 ± 1.6	−59.3 ± 5.7

[a] Equilibrium association constants (K_{as}), standard molar Gibbs free energy changes ($\Delta G°$), standard molar calorimetric enthalpy changes ($\Delta H°$), and entropy changes ($\Delta S°$) at 293 K. [b] Data from ref 47.

Table 2. Thermodynamic Parameters for Binding of Cap Analogs to Yeast eIF4E Determined by Fluorescence Titrations[a]

cap analog	K_{as} (μM^{-1})	$\Delta G°$ (kJ·mol^{-1})	$\Delta H°$ (kJ·mol^{-1})	$\Delta S°$ (J·mol^{-1}·K^{-1})
m^{7}GMP	1.01 ± 0.08	−33.73 ± 0.22	−54 ± 16	−72 ± 24
m^{7}GDP	11.87 ± 0.99	−39.68 ± 0.20		
m^{7}GTP	18.46 ± 0.83	−40.85 ± 0.10	−65.1 ± 1.8	−82.5 ± 5.9
m$_3^{2,2,7}$GTP	0.22 ± 0.01	−29.98 ± 0.11		
m^{7}GpppG	8.69 ± 0.69	−38.92 ± 0.19		
m$_2^{2,7}$GpppG	7.78 ± 0.33	−38.65 ± 0.10		
m$_3^{2,2,7}$GpppG	0.27 ± 0.02	−30.47 ± 0.18		

[a] Equilibrium association constants (K_{as}), standard molar Gibbs free energy changes ($\Delta G°$), standard molar van't Hoff enthalpy changes ($\Delta H°$), and entropy changes ($\Delta S°$) at 293 K.

m^{7}GTP, were also determined from the equilibrium binding constants at various temperatures (Table 2). Examples of calorimetric and fluorescence titration curves are shown in Figures 2 and 3, respectively. The results derived by the two independent methods are in a good agreement, i.e., in principle within the range of 3σ (Tables 1, 2). The rank order of the relative affinities expressed in terms of K_{as} for the series of cap analogs is the same. The differences in the corresponding values of the standard molar Gibbs free energies of the binding, $\Delta G°$, are less than or on the order of the characteristic energy of thermal fluctuations, RT.

Elongation of the phosphate chain of the mononucleotide mRNA 5′ cap analogs from one phosphate group (m^{7}GMP) to the diphosphate (m^{7}GDP) is accompanied by the ∼10-fold jump of the association constant and the binding free energy change, $\Delta\Delta G°$, of about −5 kJ·mol^{-1}. Further extension from two to three phosphates (m^{7}GTP) in the chain is reflected by a negligible, ∼1.5-fold, increase of K_{as} and $\Delta\Delta G°$ of about −1 kJ·mol^{-1}. The presence of the second nucleoside in the cap analog yields only a ∼2-fold decrease of K_{as} in the comparison with m^{7}GTP. The corresponding change of the binding free energy is about +1.5 kJ·mol^{-1}.

The results obtained for m^{7}GTP and m$_3^{2,2,7}$GTP show that double methylation of the N^2-amino group of the guanosine moiety results in a very substantial, ca. 80-fold, decrease of K_{as}, and a change of the binding free energy by about +10 kJ·mol^{-1}, while single methylation does not disturb the binding. Such a decrease in affinity of the trimethylguanosine cap is analogous to, although less pronounced than, that observed for murine eIF4E.[27]

Thermodynamic Parameters of Yeast eIF4E−Cap Binding. The thermodynamic parameters, $\Delta H°$ and $\Delta S°$, obtained from

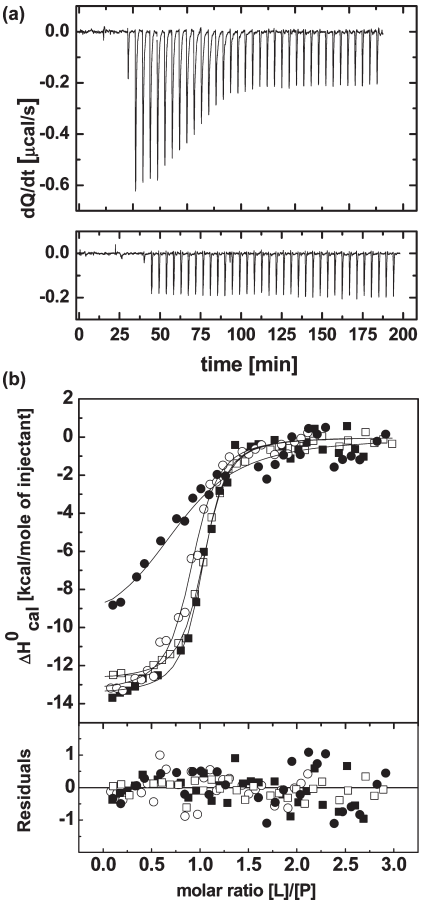

Figure 2. Isothermal titration calorimetry measurements for interactions of yeast eIF4E with m^{7}GMP (●), m^{7}GDP (○), m^{7}GTP (■), and m^{7}GpppG (□), at 293 K: (a) example of raw data; (b) binding isotherms fitted to integrated heat signals.

calorimetric and spectroscopic experiments are gathered in Tables 1 and 2, respectively. Though the fluorescence and calorimetric titrations were run at the protein concentrations that differed by 20−67-fold, the thermodynamic results yielded by ITC and the van't Hoff method are coherent. Interactions of all monomethylguanosine cap analogs with yeast eIF4E are enthalpy-favorable and entropy-opposed at 293 K. However, the negative entropic contribution is not very high; thus the value of the Gibbs free energy in relation to the binding enthalpy, $\Delta G°/\Delta H°$, is always greater than 65%.

The calorimetric standard molar enthalpy changes of the complex formation for m^{7}GDP, m^{7}GTP, and m^{7}GpppG are close to each other and are more negative than $\Delta H°_{cal}$ for m^{7}GMP by about 18 kJ·mol^{-1}. Similarly, the calorimetrically determined standard molar entropy changes for m^{7}GDP, m^{7}GTP, and m^{7}GpppG are almost equal (within the experimental error) and differ from the m^{7}GMP binding entropy by about −43 J·mol^{-1}·K^{-1}.

Fluorescence titrations at different temperatures shown in Figure 4 reveal that the association constant for m^{7}GTP decreases monotonically with temperature, while K_{as} for the low affinity ligand, m^{7}GMP, attains a minimum at 303 K and further slightly increases (Table 3). The van't Hoff analyses (Figure 5) show that interaction of the yeast eIF4E with m^{7}GMP is described better by a nonlinear dependence of ln K_{as} vs $1/T$ (eq 5), with the P value of 0.026 in the Snedecor's F-test,[48] contrary to the highest affinity ligand, m^{7}GTP.

dx.doi.org/10.1021/jp2012039 |J. Phys. Chem. B 2011, 115, 8746–8754

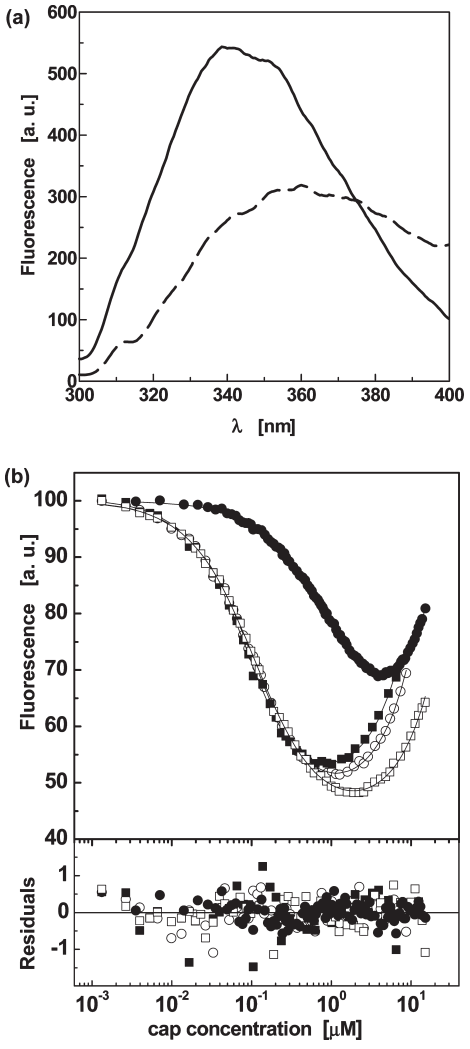

Figure 3. (a) Fluorescence spectra of yeast eIF4E before and after titration by a cap analog. (b) Binding isotherms fitted to titration data for m^7GMP (●), m^7GDP (○), m^7GTP (■), and m^7GpppG (□), at 293 K. The increase of the fluorescence signal toward the end of titrations results from the presence of free fluorescent ligand molecules in the solution.

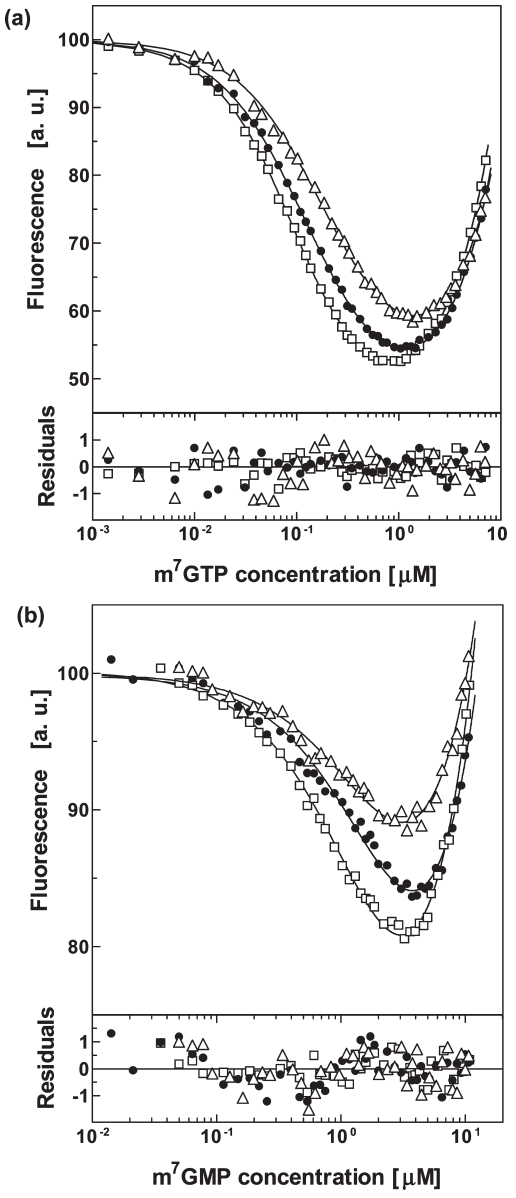

Figure 4. Fluorescence binding isotherms for association of yeast eIF4E with (a) m^7GTP and (b) m^7GMP, at 298 K (□), 303 K (●), and 308 K (Δ). The association constant is related to the ligand concentration at which saturation occurs, not to the quenching intensity at given temperature.

The resulting nonzero standard molar heat capacity change that accompanies the m^7GMP binding has a positive sign, $\Delta C_p^\circ = +5.2 \pm 1.3$ kJ·mol^{-1}·K^{-1}. The critical temperatures at which ΔH_{vH}° and ΔS° attain zero are $T_H = 303.7 \pm 1.6$ K and $T_S = 297.3 \pm 0.9$ K, respectively. A similar effect for low affinity ligands ($m_3^{2,2,7}$GTP, m^7GMP, m^7GpppC, m^7GpppG, m^7Gpppp(m^7G)) was previously observed and exhaustively discussed for the murine eIF4E.[32,38] The van't Hoff enthalpy change of the yeast eIF4E binding to m^7GTP at 293 K is significantly more negative than that for m^7GMP, with the corresponding difference between the standard molar entropy changes (Table 2), in agreement with the calorimetric results (Table 1).

It is worth noting that the van't Hoff and calorimetric results are highly concordant, although these two methodological approaches are sensitive to different variable parameters describing reactions in solution. Fluorescence titrations reflect local environment changes of tryptophan indole rings, which correspond only to direct fluorescence quenching or dark complex formation by ligands in protein active sites, and to protein conformational changes due to ligand binding. In contrast, ITC is incapable of measuring the net effect related only to protein–ligand interaction but detects the total heat signal cumulated from all reactions taking place concurrently in the reaction cell, including accompanying processes, in particular, coupled ion exchange, hydration changes, protonation changes, and possible precipitation.

The only one discrepancy exceeding 3σ between the calorimetrically and spectroscopically determined thermodynamic parameters is related to the m^7GTP binding enthalpy, $\Delta H_{cal}^\circ - \Delta H_{vH}^\circ = +8.8 \pm 1.9$ kJ·mol^{-1}. This value is close to the HEPES ionization heat, $\Delta H_{ion}^\circ = +6.9$ kJ·mol^{-1},[45] which should be released at pH 7.2 when the cap analog characterized by $pK_a = 7.5$ is partially protonated from the zwitterionic to cationic form. A similar shift of ΔH_{cal}° toward

dx.doi.org/10.1021/jp2012039 |J. Phys. Chem. B 2011, 115, 8746–8754

Table 3. Equilibrium Association Constants (K_{as}) for Binding of m^{7}GMP and m^{7}GTP to Yeast eIF4E Determined by Fluorescence Titrations at Different Temperatures

	K_{as} (μM^{-1})	
T (K)	m^{7}GMP	m^{7}GTP
314	0.663 ± 0.050	3.26 ± 0.19
308	0.608 ± 0.042	5.37 ± 0.54
303	0.442 ± 0.017	8.18 ± 0.44
298	0.566 ± 0.026	14.89 ± 1.11
293	0.931 ± 0.088	19.18 ± 0.81
288	1.133 ± 0.036	30.08 ± 0.75

the more positive value in relation to ΔH°_{vH} is also observed for m^{7}GMP, although the experimental uncertainty of the parameters determined from the van't Hoff method does not allow strict interpretation for that case. Overall, the comparison of the enthalpy values suggests that yeast eIF4E stabilizes the positively charged 7-methylguanosine moiety of the cap, similarly as it was found for the mammalian protein.[26,27,38]

Isothermal Enthalpy−Entropy Compensation. A great deal of work has been reported on isothermal enthalpy−entropy compensation but the interpretation of this phenomenon is controversial.[49] In the majority of cases such compensation can be explained as a trivial interplay between enthalpic and entropic contributions to interactions measured for congener series characterized by a single source of additivity, e.g., build by repetition of the same chemical group. Such compensation yields usually a very low value of ΔG° in comparison with the corresponding ΔH°, and a characteristic compensation temperature, T_c, defined from a slope of the $T\Delta S^{\circ}$ vs ΔH° relationship is usually indiscernible from the mean temperature of the experiment.[49] A criterion for validation of a nontrivial isothermal enthalpy−entropy compensation, which can be thus interpreted in terms of conformational changes accompanying the interaction, was proposed as a statistically important difference between the harmonic mean of experimental temperatures and T_c.[50,51]

The compensation temperature resulting from the calorimetric enthalpy and entropy changes for yeast eIF4E (Table 1, Figure 6) is equal to $T_c = 411 \pm 18$ K, which is greater than 4σ from the experimental temperature of 293 K. This result is close to those found previously for the mouse protein ($T_c = 399 \pm 24$ K[32]) and can be ascribed to silencing of the protein structural fluctuations upon the cap binding, which corresponds to the internal energy difference by about 8.5 kJ/mol. This means that the overall, minor conformational changes leading to structural stiffening of the 4E translation initiation factor upon binding to the mRNA 5′ cap is similar for both yeast and mammals.[32] The specific regions of human[34] and mouse[35] eIF4E influenced upon the m^{7}GTP binding have been identified by NMR and hydrogen/deuterium exchange kinetics, respectively, pointing not only at the fragments encompassing the cap binding site but also at the distant molecule regions related to protein−protein interactions with another initiation factor, eIF4G, and translation inhibitors, 4E-BPs.

Differences and Similarities in Interactions of the mRNA 5′ Cap with Yeast and Murine eIF4Es. Comparison of the mammalian and yeast eIF4E 3D structures[26−29] reveals high conformational dynamics of the m^{7}GDP phosphate chain in the complex with the yeast factor. This is expressed by substantially greater relative standard square deviations, SD^2, of the phosphorus and oxygen atoms compared with the SD^2 of the remaining heavy atoms of the

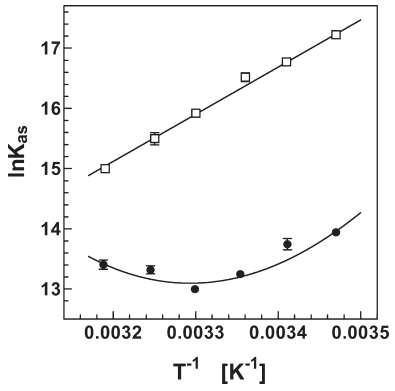

Figure 5. Thermodynamics of yeast eIF4E interaction with the mRNA 5′ cap analogs described by the van't Hoff plot in a linear (eq 4) or nonlinear form (eq 5) for m^{7}GTP (□) and m^{7}GMP (●), respectively.

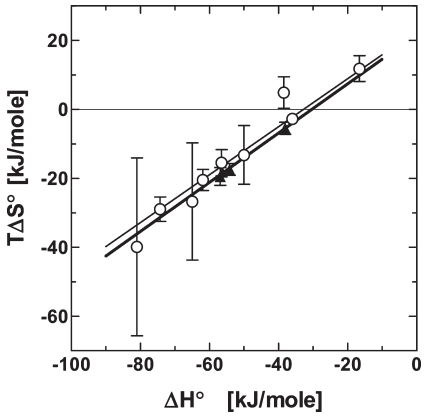

Figure 6. Isothermal enthalpy−entropy compensation for a series of cap analogs upon their interaction with eIF4E from yeast (▲) and mouse[33] (○) at 293 K.

cap bound to yeast eIF4E, calculated for the 20 lowest energy NMR structures (Figure 7a). In contrast, similar inspection of a parameter that is a crystallographic counterpart of SD^2 derived from NMR, i.e., the relative mean square displacement, u^2, which is proportional to the crystallographic temperature B factor of the m^{7}GDP atoms in the murine eIF4E complex, shows much better stability of the phosphate chain conformation (Figure 7b).

Comparing the dynamic aspects of mammalian and yeast eIF4E structures, one should keep in mind methodological differences in the structure determination by X-ray diffraction vs NMR in solution. The set of the lowest energy NMR solution structures is obtained by means of a simulated annealing protocol.[52] The molecular dynamics programs used to refine solution structures exploit a simple mechanical force-field with repulsion terms and NMR constraints as the nonbonded interactions. If the number of the constraints for some parts of a molecule, e.g., the residues interacting with the phosphate chain of the cap, was too small, the structure could be undefined in these parts due to oversimplification of the electrostatic potential. However, in the case of a relatively large (from the NMR point of view) molecular system like the yeast eIF4E-m^{7}GDP complex[29] (PDB 1ap8), the structural dynamics of the bound ligand revealed by the 20 lowest energy structures inevitably correlates with the dynamics of the surrounding protein residues. Hence,

dx.doi.org/10.1021/jp2012039 |J. Phys. Chem. B 2011, 115, 8746–8754

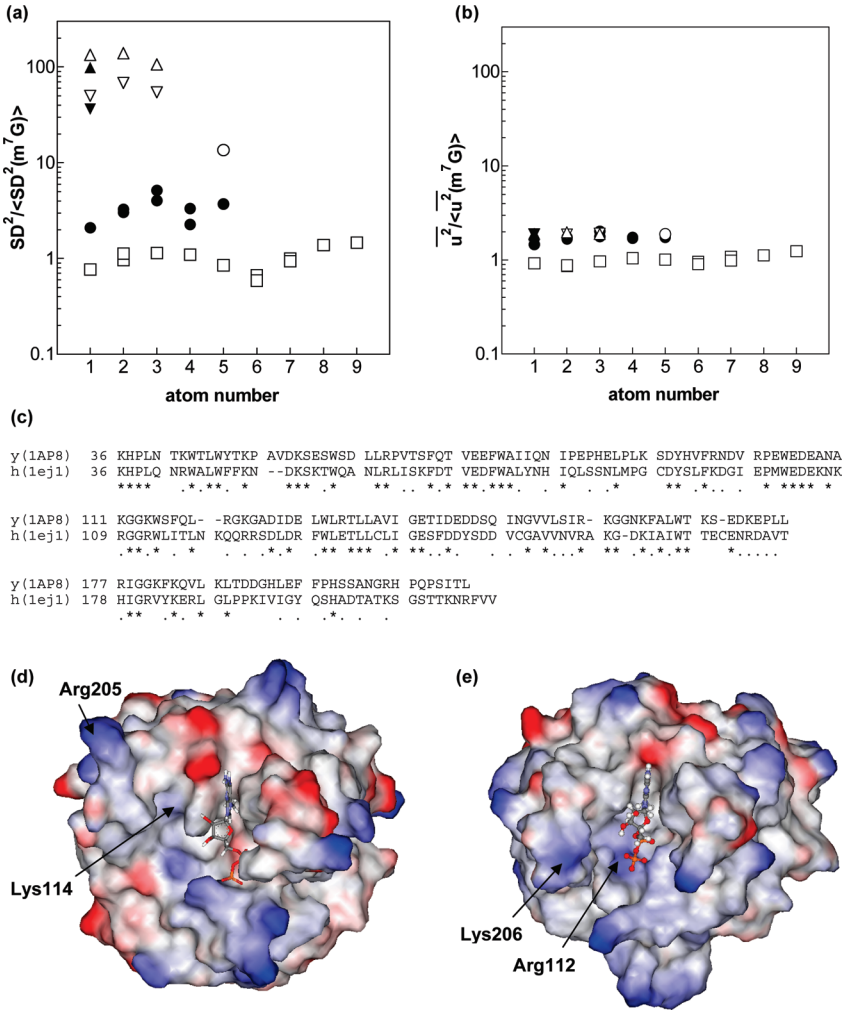

Figure 7. (a) Relative standard square deviations, SD^2, of the m^7GDP heavy atoms in the complex with yeast eIF4E, calculated for 20 NMR structures (PDB 1ap8[29]), normalized to the average value for the 7-methylguanosine ring atoms, $\langle SD^2(m^7G)\rangle$. (b) Relative mean square displacements, $\overline{u^2}$, of the m^7GDP heavy atoms in the crystallographic complex with mouse eIF4E (PDB 1ej1[26]), normalized to the average value for the 7-methylguanosine ring atoms, $\langle \overline{u^2}(m^7G)\rangle$. The 7-methylguanosine base (□) and ribose (●) atoms are numbered according to Figure 1. Other atoms are marked as follows: $O5'$ (○), P_α (▼), O_α (▽), P_β (▲), and O_β (△). (c) Sequence alignment according to structural alignment for the C^α atoms of the representative yeast eIF4E (1ap8[29]) OLDERADO structure[46] and mouse eIF4E crystal structure (1ej1[26]). Molecular electrostatic potential surface of (d) the yeast and (e) murine eIF4E. Both surfaces are in the same projection resulting from the structural C^α alignment.

the number of the constraints for this protein−ligand complex seems to be great enough to define the structural dynamics of the complex as a whole. Therefore, one may conclude that the conformational instability of the cap phosphate chain bound to yeast eIF4E reflects a real effect and not a methodological artifact.

The sequence alignments do not provide any simple clue to elucidate this difference in conformational dynamics, because the key basic amino acids are strictly conserved among species (Figure 7c). However, the spatial orientation of these residues has changed evolutionarily by mutations in nonconserved regions to accommodate the positively charged groups closer to the cap phosphate chain. The arrangement of the basic amino acid side chains in yeast (Figure 7d) and mouse (Figure 7e) eIF4E shows that in yeast, contrary to mammals, the lysines and arginines do not form a compact, positively charged cluster at the entrance to the cap-binding pocket. Two basic residues, Arg205 and Lys114, which correspond to Lys206 and Arg112 in the murine eIF4E, are too far apart to make efficient stabilizing contacts with the cap phosphate chain.

Yeast eIF4E binds to the mononucleotide cap analogs with shorter phosphate chains and to $m_3^{2,2,7}GTP$ with the same affinity as the mammalian protein, but to 7-methylguanosine triphosphate with the association constant by an order of magnitude lower.[32] This difference corresponds to the binding free energy difference of about 5−6 kJ/mol, which is a typical value of a single hydrogen bond or a salt bridge formed between a protein and a ligand in buffered milieu.[53−55] Accordingly, the van't Hoff binding enthalpy for the interaction of the yeast eIF4E with m^7GTP is by about +10 kJ/mol less negative than that for mouse eIF4E,[32] which suggests that eIF4E adopted a more enthalpic binding mechanism in higher organisms.[32,38] Hence, while a general view of the cap binding by yeast eIF4E is similar to the molecular mechanism proposed for mammalian proteins,[27,32,34,35,38,56,57] the almost equal affinity of yeast eIF4E for m^7GDP and m^7GTP is in contrast with mammalian eIF4E for which interatomic contacts between the γ-phosphate of the cap and the positively charged amino acid side chains provide a key contribution to the free energy of the complex stabilization.[27,58,59] This is expressed by the ca. 5-fold greater

association constant for m^7GTP than for m^7GDP, 108.7 ± 4.0 μM^{-1} vs 20.4 ± 1.5 μM^{-1}, respectively, which corresponds to the decrease of the Gibbs free energy of binding by about $\Delta\Delta G^\circ = -4.10 \pm 0.21$ kJ/mol,[27] a value typical for one additional noncovalent hydrogen bond or salt bridge in a polar solvent and in the presence of electrolytic screening by the solution components.[60] The enthalpic contribution, $\Delta\Delta H^\circ$, to the binding of the γ-phosphate of the cap by murine eIF4E is significant and equals −12.4 ± 4.6 kJ/mol.[32]

The interactions with the cap phosphate chain are established at the outer, solvent-accessible protein surface, close to the entrance to the 7-methylguanosine binding slot. This suggests that the improvement of the m^7GTP complex stability for mammalian proteins could be obtained only by changes of the spatial positions of the positively charged residues, while the main conformational "hinge lock" mechanism[34] that leads to formation of the tight hydrophobic-aromatic cap-binding pocket involving Trp56 and Trp102 can be similar for yeast and mammals. This conclusion is supported by the similarity of the enthalpy−entropy compensation relationships for yeast and mouse (Figure 6).

Biological Consequences. The eukaryotic 4E initiation factor plays a key role in many aspects of post-transcriptional gene expression,[61,62] and various mechanisms are utilized in regulation of its activity.[63] According to the two-step model of the mammalian eIF4E−cap complex formation,[27,57] the incoming cap is tightly anchored by the triphosphate bridge and further stabilized by cooperative formation of the sandwich cation−π stacking and hydrogen bonding of the 7-methylguanosine moiety.

Evolution of the eIF4E amino acid sequence, from yeast to mammals, seems to proceed toward assemblage or "clustering" of positively charged lysines and arginines at the entrance of the m^7G-binding slot. These basic amino acids are strictly conserved along the sequence (Figure 7c), but their spatial orientations have changed by mutations in nonconserved regions to accommodate more favorable arrangement of the positively charged groups (Figure 7e), thus enabling the formation of one additional noncovalent intermolecular contact involving the γ-phosphate group in mammals. This is an interesting example of acquiring a greater efficacy of complex stabilization via mutations in those regions of the protein sequence that are not engaged in direct, specific ligand binding through formation of interatomic contacts. Such a mechanism enables soft-tuning of a protein structure to bind ligands more effectively without loosing the biological functionality of the protein related to the highly conserved amino acids.

CONCLUSIONS

Thermodynamic analysis of the interactions of yeast eIF4E with the mRNA 5′ cap analogs by ITC and the van't Hoff method revealed an electrostatic mechanism of the affinity enhancement in the yeast, compared to mammals. The chemical cap analogs with smaller charge at the phosphate chain are recognized by the yeast eIF4E with similar affinity as by the mammalian proteins, while the complex with m^7GTP is stabilized significantly less tightly than that for human or mouse eIF4E. The binding enhancement in mammalian proteins is attained by spatial rearrangement of strictly conserved positively charged amino acid side chains to be more focused around the entrance to the cap-binding slot in comparison with the yeast protein. The nontrivial isothermal enthalpy−entropy compensation shows that the overall protein conformational changes that accompany the cap binding are similar for yeast and mouse eIF4E.

AUTHOR INFORMATION

Corresponding Author

*Phone: +48 22 843 66 01. Fax: +48 22 843 09 26. E-mail: annan@ifpan.edu.pl.

ACKNOWLEDGMENT

We thank Prof. W. Zielenkiewicz and Dr. M. Wszelaka-Rylik for excellent assistance at ITC, Prof. T. Preiss for the yeast eIF4E plasmid, Dr. Joanna Trylska for critical reading of the manuscript, and the Polish Ministry of Science and Higher Education (N N301 267137 to A.N.; N N301 035936 to A.M.W., R.S., N N301 096339 to E.D., J.S.) and the HHMI (55005604 to E.D.) for financial support.

ABBREVIATIONS

eIF4E, eukaryotic initiation factor 4E; m^7GMP, 7-methylguanosine monophosphate; m^7GDP, 7-methylguanosine diphosphate; m^7GTP, 7-methylguanosine triphosphate; $m_3^{2,2,7}GTP$, N^2,N^2,7-trimethylguanosine-5′ triphosphate; m^7GpppG, P^1-7-methylguanosine-5′-P^3-guanosine-5′ triphosphate; $m_2^{2,7}GpppG$, P^1- N^2,7-dimethylguanosine-5′-P^3-guanosine-5′ triphosphate; $m_3^{2,2,7}GpppG$, P^1-N^2,N^2,7-trimethylguanosine-5′-P^3-guanosine-5′ triphosphate; EDTA, ethylenediaminetetraacetic acid; HEPES, 4-(2-hydroxyethyl)-1-piperazineethanesulfonic acid; σ, standard deviation

REFERENCES

(1) Alberty, R. A. *J. Phys. Chem. B* **2010**, *114*, 17003–17012.
(2) Record, M. T., Jr.; Ha, J. H.; Fisher, M. A. *Methods Enzymol.* **1991**, *208*, 291–343.
(3) Naghibi, H.; Tamura, A.; Sturtevant, J. M. *Proc. Natl. Acad. Sci. U. S. A.* **1995**, *92*, 5597–5599.
(4) Liu, Y.; Sturtevant, J. M. *Protein Sci.* **1995**, *4*, 2559–2561.
(5) Liu, Y.; Sturtevant, J. M. *Biophys.Chem.* **1997**, *64*, 121–126.
(6) Fiedor, J.; Pilch, M.; Fiedor, L. *J. Phys. Chem. B* **2009**, *113*, 12831–12838.
(7) Wang, S. H.; Liu, F. F.; Dong, X. Y.; Sun, Y. *J. Phys. Chem. B* **2010**, *114*, 11576–11583.
(8) Persson, B. A.; Jonsson, B.; Lund, M. *J. Phys. Chem. B* **2009**, *113*, 10459–10464.
(9) Muthukrishnan, S.; Both, G. W.; Furuichi, Y.; Shatkin, A. J. *Nature* **1975**, *255*, 33–37.
(10) Van Doren, K.; Hirsh, D. *Mol. Cell. Biol.* **1990**, *10*, 1769–1772.
(11) Miyoshi, H.; Dwyer, D. S.; Keiper, B. D.; Jankowska-Anyszka, M.; Darzynkiewicz, E.; Rhoads, R. E. *EMBO J.* **2002**, *21*, 4680–4690.
(12) Stachelska, A.; Wieczorek, Z.; Ruszczynska, K.; Stolarski, R.; Pietrzak, M.; Lamphear, B. J.; Rhoads, R. E.; Darzynkiewicz, E.; Jankowska-Anyszka, M. *Acta Biochim. Pol.* **2002**, *49*, 671–682.
(13) Lall, S.; Friedman, C. C.; Jankowska-Anyszka, M.; Stepinski, J.; Darzynkiewicz, E.; Davis, R. E. *J. Biol. Chem.* **2004**, *279*, 45573–45585.
(14) Liu, W. Z.; Zhao, R.; McFarland, C.; Kieft, J.; Niedzwiecka, A.; Jankowska-Anyszka, M.; Stepinski, J.; Darzynkiewicz, E.; Jones, D. N. M.; Davis, R. E. *J. Biol. Chem.* **2009**, *284*, 31336–31349.
(15) Gingras, A. C.; Raught, B.; Sonenberg, N. *Annu. Rev. Biochem.* **1999**, *68*, 913–963.
(16) Varani, G. *Structure* **1997**, *5*, 855–858.
(17) Konarska, M. M.; Padgett, R. A.; Sharp, P. A. *Cell* **1984**, *38*, 731–736.
(18) Hamm, J.; Darzynkiewicz, E.; Tahara, S. M.; Mattaj, I. W. *Cell* **1990**, *62*, 569–577.
(19) Raught, B.; Gingras, A. C. *Int. J. Biochem. Cell Biol.* **1999**, *31*, 43–57.
(20) Culjkovic, B.; Topisirovic, I.; Borden, K. L. B. *Cell Cycle* **2007**, *6*, 65–69.

(21) Sonenberg, N. *Translational Control*; CSHL Press: Cold Spring Harbor, NY, 1996; pp 245−269.
(22) Lazaris-Karatzas, A.; Montine, K. S.; Sonenberg, N. *Nature* **1990**, *345*, 544–547.
(23) De Benedetti, A.; Graff, J. R. *Oncogene* **2004**, *23*, 3189–3199.
(24) Graff, J. R.; Konicek, B. W.; Vincent, T. M.; Lynch, R. L.; Monteith, D.; Weir, S. N.; Schwier, P.; Capen, A.; Goode, R. L.; Dowless, M. S.; Chen, Y.; Zhang, H.; Sissons, S.; Cox, K.; McNulty, A. M.; Parsons, S. H.; Wang, T.; Sams, L.; Geeganage, S.; Douglass, L. E.; Neubauer, B. L.; Dean, N. M.; Blanchard, K.; Shou, J.; Stancato, L. F.; Carter, J. H.; Marcusson, E. G. *J. Clin. Invest.* **2007**, *117*, 2638–2648.
(25) Morley, S. J.; Curtis, P. S.; Pain, V. M. *RNA* **1997**, *3*, 1085–1104.
(26) Marcotrigiano, J.; Gingras, A. C.; Sonenberg, N.; Burley, S. K. *Cell* **1997**, *89*, 951–961.
(27) Niedzwiecka, A.; Marcotrigiano, J.; Stepinski, J.; Jankowska-Anyszka, M.; Wyslouch-Cieszynska, A.; Dadlez, M.; Gingras, A. C.; Mak, P.; Darzynkiewicz, E.; Sonenberg, N.; Burley, S. K.; Stolarski, R. *J. Mol. Biol.* **2002**, *319*, 615–635.
(28) Tomoo, K.; Shen, X.; Okabe, K.; Nozoe, Y.; Fukuhara, S.; Morino, S.; Ishida, T.; Taniguchi, T.; Hasegawa, H.; Terashima, A.; Sasaki, M.; Katsuya, Y.; Kitamura, K.; Miyoshi, H.; Ishikawa, M.; Miura, K. *Biochem. J.* **2002**, *362*, 539–544.
(29) Matsuo, H.; Li, H.; McGuire, A. M.; Fletcher, C. M.; Gingras, A. C.; Sonenberg, N.; Wagner, G. *Nat. Struct. Biol.* **1997**, *4*, 717–724.
(30) Monzingo, A. F.; Dhaliwal, S.; Dutt-Chaudhuri, A.; Lyon, A.; Sadow, J. H.; Hoffman, D. W.; Robertus, J. D.; Browning, K. S. *Plant Physiol.* **2007**, *143*, 1504–1518.
(31) Niedzwiecka, A.; Darzynkiewicz, E.; Stolarski, R. *J. Phys.: Condens. Matter* **2005**, *17*, S1483–S1494.
(32) Niedzwiecka, A.; Darzynkiewicz, E.; Stolarski, R. *Biochemistry* **2004**, *43*, 13305–13317.
(33) Tomoo, K.; Shen, X.; Okabe, K.; Nozoe, Y.; Fukuhara, S.; Morino, S.; Sasaki, M.; Taniguchi, T.; Miyagawa, H.; Kitamura, K.; Miura, K.; Ishida, T. *J. Mol. Biol.* **2003**, *328*, 365–383.
(34) Volpon, L.; Osborne, M. J.; Topisirovic, I.; Siddiqui, N.; Borden, K. L. B. *EMBO J.* **2006**, *25*, 5138–5149.
(35) Rutkowska-Wlodarczyk, I.; Stepinski, J.; Dadlez, M.; Darzynkiewicz, E.; Stolarski, R.; Niedzwiecka, A. *Biochemistry* **2008**, *47*, 2710–2720.
(36) von der Haar, T.; Oku, Y.; Ptushkina, M.; Moerke, N.; Wagner, G.; Gross, J. D.; McCarthy, J. E. G. *J. Mol. Biol.* **2006**, *356*, 982–992.
(37) McCubbin, W. D.; Edery, I.; Altmann, M.; Sonenberg, N.; Kay, C. M. *J. Biol. Chem.* **1988**, *263*, 17663–17671.
(38) Niedzwiecka, A.; Stepinski, J.; Darzynkiewicz, E.; Sonenberg, N.; Stolarski, R. *Biochemistry* **2002**, *41*, 12140–12148.
(39) Darzynkiewicz, E.; Ekiel, I.; Tahara, S. M.; Seliger, L. S.; Shatkin, A. J. *Biochemistry* **1985**, *24*, 1701–1707.
(40) Jankowska, M.; Stepinski, J.; Stolarski, R.; Temeriusz, A.; Darzynkiewicz, E. *Collect. Czech. Chem. Commun.* **1993**, *58*, 138–141.
(41) Stepinski, J.; Bretner, M.; Jankowska, M.; Felczak, K.; Stolarski, R.; Wieczorek, Z.; Cai, A. L.; Rhoads, R. E.; Temeriusz, A.; Haber, D.; Darzynkiewicz, E. *Nucleos. Nucleot.* **1995**, *14*, 717–721.
(42) Ruszczynska, K.; Kamienska-Trela, K.; Wojcik, J.; Stepinski, J.; Darzynkiewicz, E.; Stolarski, R. *Biophys. J.* **2003**, *85*, 1450–1456.
(43) Niedzwiecka A.; Stepinski, J.; Antosiewicz, J. M.; Darzynkiewicz, E.; Stolarski, R. Translation Initiation: Reconstituted Systems and Biophysical Methods. *Methods in Enzymology*; Elsevier: Amsterdam, 2007; Chapter 9, pp 209−245.
(44) Baldwin, R. L. *Proc. Natl. Acad. Sci. U. S. A.* **1986**, *83*, 8069–8072.
(45) Christensen, J. J.; Hansen, L. D.; Izatt, R. M. *Handbook of proton ionization heats and related thermodynamic quantities*; John Wiley & Sons: New York, 1976.
(46) Kelley, L. A.; Sutcliffe, M. J. *Protein Sci.* **1997**, *6*, 2628–2630.
(47) Kiraga-Motoszko, K.; Stepinski, J.; Niedzwiecka, A.; Jemielity, J.; Wszelaka-Rylik, M.; Stolarski, R.; Zielenkiewicz, W.; Darzynkiewicz, E. *Nucleosides, Nucleotides Nucleic Acids* **2003**, *22*, 1711–1714.
(48) Beyer, W. H. *CRC Standard mathematical tables*, 28th ed.; CRC Press: Boca Raton, FL, 1987; p 536.
(49) Sharp, K. *Protein Sci.* **2001**, *10*, 661–667.
(50) Krug, R. R.; Hunter, W. G.; Grieger, R. A. *J. Phys. Chem.* **1976**, *80*, 2335–2341.
(51) Krug, R. R.; Hunter, W. G.; Grieger, R. A. *Nature* **1976**, *261*, 566–567.
(52) Nilges, M.; Clore, G. M.; Gronenborn, A. M. *FEBS Lett.* **1988**, *239*, 129–136.
(53) Horovitz, A.; Serrano, L.; Avron, B.; Bycroft, M.; Fersht, A. R. *J. Mol. Biol.* **1990**, *216*, 1031–1044.
(54) Pace, C. N.; Shirley, B. A.; McNutt, M.; Gajiwala, K. *FASEB J.* **1996**, *10*, 75–83.
(55) Kuntz, I. D.; Chen, K.; Sharp, K. A.; Kollman, P. A. *Proc. Natl. Acad. Sci. U. S. A.* **1999**, *96*, 9997–10002.
(56) Niedzwiecka-Kornas, A.; Chlebicka, L.; Stepinski, J.; Jankowska-Anyszka, M.; Wieczorek, Z.; Darzynkiewicz, E.; Rhoads, R. E.; Stolarski, R. *Collect. Symp. Ser.* **1999**, *2*, 214–218.
(57) Blachut-Okrasinska, E.; Bojarska, E.; Niedzwiecka, A.; Chlebicka, L.; Darzynkiewicz, E.; Stolarski, R.; Stepinski, J.; Antosiewicz, J. M. *Eur. Biophys. J.* **2000**, *29*, 487–498.
(58) Zuberek, J.; Wyslouch-Cieszynska, A.; Niedzwiecka, A.; Dadlez, M.; Stepinski, J.; Augustyniak, W.; Gingras, A. C.; Zhang, Z.; Burley, S. K.; Sonenberg, N.; Stolarski, R.; Darzynkiewicz, E. *RNA* **2003**, *9*, 52–61.
(59) Zuberek, J.; Jemielity, J.; Jablonowska, A.; Stepinski, J.; Dadlez, M.; Stolarski, R.; Darzynkiewicz, E. *Biochemistry* **2004**, *43*, 5370–5379.
(60) Bloomfield, V. A. *Biophysics Textbook online*; Biophysical Society & IUPAB: Rockville, MD, 2001.
(61) von der Haar, T.; Gross, J. D.; Wagner, G.; McCarthy, J. E. G. *Nat. Struct. Mol. Biol.* **2004**, *11*, 503–511.
(62) Richter, J. D.; Sonenberg, N. *Nature* **2005**, *433*, 477–480.
(63) Raught, B.; Gingras, A. C.; Sonenberg, N. *Translational Control of Gene Expression*; Cold Spring Harbor Laboratory Press: New York, 2000; pp 245−293.